

# Optimal Control Utilizing Analytical Solutions for Heavy Truck Cruise Control

LiTH-ISY-R-2842  
Anders Fröberg and Lars Nielsen  
Linköpings Universitet  
SE-581 83 Linköping, Sweden

April 4, 2008

## Abstract

The problem addressed is how to control vehicle speed over a given distance on a given time such that fuel consumption is minimized. Analytical expressions for the necessary optimality conditions are derived. These expressions are essential for the understanding of the decisive parameters affecting fuel optimal driving and the analytical optimality conditions make it possible to see how each parameter affects the optimal solution. Optimal solutions for an affine engine torque model are compared to solutions for a piece-wise affine model, and it is shown that small non-linearities have significant effect on the optimal control strategy. The solutions for the non linear engine model has a smoother character but also requires longer prediction horizons.

Assuming a continuously variable transmission, optimal gear ratio control is presented, and it is shown how the maximum fueling function is essential for the solution. It is also shown that the gear ratio never is chosen such that engine speed exceeds the speed of maximum engine power. Those results are then extended to include a discrete stepped transmission, and it is demonstrated how gear shifting losses affect optimal gear shifting positions.

The theory presented is a good base to formalize the intuition of fuel efficient driving. To show this, optimal solutions are presented in simulations of some constructed test road profiles, where the typical behavior of an optimal solution is pointed out, and also which parameters that are decisive for the fuel minimization problem. This is then used to design a simple low-complexity computationally efficient rule-based look ahead cruise controller, and it is demonstrated that simple parametrized quantitative rules have potential for significant fuel savings.



# Contents

<b>1</b>	<b>Introduction</b>	<b>5</b>
<b>2</b>	<b>Problem formulation</b>	<b>6</b>
<b>3</b>	<b>Optimal fueling -Affine engine characteristics</b>	<b>6</b>
3.1	Solution characteristics . . . . .	9
<b>4</b>	<b>PWA engine characteristics</b>	<b>11</b>
4.1	Concave engine map . . . . .	12
4.2	Non concave engine map . . . . .	12
4.3	Non linear engine speed characteristics . . . . .	13
<b>5</b>	<b>Optimal gear ratio control</b>	<b>14</b>
5.1	Optimal gear ratio - affine maximum fueling . . . . .	14
5.2	Optimal gear ratio - quadratic maximum fueling . . . . .	16
5.3	Discrete step transmission . . . . .	19
5.4	Optimal gear ratio for PWA engine characteristics . . . . .	20
<b>6</b>	<b>Simulations</b>	<b>21</b>
6.1	Optimal solutions for uphill and downhill slopes . . . . .	22
6.2	Affine and piece-wise affine modeling . . . . .	22
6.3	Continuously variable gear ratio optimization . . . . .	24
6.4	Discrete stepped transmission . . . . .	26
6.5	Interpretation of the Lagrange variables . . . . .	26
6.6	Speed limits . . . . .	27
6.7	Discussion . . . . .	28
<b>7</b>	<b>Sensitivity analysis</b>	<b>28</b>
<b>8</b>	<b>Rule based predictive cruise control</b>	<b>31</b>
8.1	Optimization criterion . . . . .	31
8.2	On-line algorithm . . . . .	33
<b>9</b>	<b>Conclusions</b>	<b>34</b>



# 1 Introduction

Fuel cost is a large part of the operating cost of heavy trucks. Hence there has been an increasing interest in predictive cruise controllers that minimize fuel consumption [18, 6, 10]. Some early work in finding fuel optimal speed profiles for automobiles is reported in [15, 7]. Other related work regarding passenger cars in urban traffic has shown on a large potential to use speed control to minimize fuel consumption [13]. Similar methods as discussed in this paper has earlier been used on rail vehicles [12].

The scenario studied here concerns heavy trucks used for long haulage and the goal is to control vehicle speed over a given distance on a given time such that fuel consumption is minimized. It is assumed that road topography ahead of the vehicle is known and the resulting problem will be referred to as look ahead cruise control. In a practical case road topography can be extracted using for example a navigation system with 3D maps or collected data. The differences between optimal solutions for a linear engine torque model and a non linear engine torque model is investigated. The non linear model is here modeled as a piece wise affine, PWA, function. Optimal gear shifting is also studied, both with a simplified transmission model with continuously variable gear ratio, and for a discrete step transmission.

Based on the modeling, the optimality conditions for the fuel minimization problem become analytical expressions. From these expressions the effect of each parameter can be studied which is important to gain knowledge of what factors that affect fuel consumption. For example, the optimal control derived here can be used as an aid when analyzing and validating the behavior of numerical controllers as described in [4] and [5]. The results are also the basis for formalizing an intuitive optimal driving behavior which can be used for design of simple rule based controllers. In this paper the effect of other traffic is not explicitly considered. However, one way to handle such situations is to consider other traffic as an extra constraint on vehicle speed. In [16] a method is presented that optimizes vehicle speed when approaching a slower vehicle.

The paper is organized as follows. The fuel minimization problem is formulated in Section 2. Under the assumption of an affine engine torque model and a fixed gear ratio, necessary conditions for optimal fueling is derived in Section 3. In Section 4 a piece-wise affine, PWA, model is used to capture the non linearities in the engine characteristics. Assuming a continuously variable transmission, optimal gear ratio is derived in Section 5 and the results are then extended to include a discrete stepped transmission. The optimality conditions for the different modeling choices are used to find optimal solutions for a few illustrative constructed road profiles, and simulation results are presented in Section 6. It is also demonstrated in Section 8 that the derived expressions can be used to design a low-complexity computationally efficient rule-based look ahead cruise controller.

## 2 Problem formulation

The problem to be solved is to minimize fuel consumption over a given distance  $s_f$  with specified travel time  $T_t$ . With notation according to Table 1 this is written as

$$\min \int_0^{s_f} \frac{\delta n_{cyl} i}{2\pi n_r r} ds \quad (1)$$

$$\text{s.t.} \quad \int_0^{s_f} \frac{1}{v} ds = T_t \quad (2)$$

The vehicle is modeled as in [3], and [9], and can be written as

$$\dot{v} = \frac{1}{J} (F_{prop} - F_{air} - F_{roll} - F_{slope} - F_b) \quad (3)$$

where the variables and parameters are selected according to Table 1, and the forces and inertias are set according to Table 2. Losses in different parts of the driveline are easily modeled as lumped losses by modifying the coefficients of engine friction losses and vehicle resistance forces. Measured engine torque from a real engine is given in Figure 1. It is there seen that an affine model of engine torque is a good first approximation, but for a detailed analysis the non linearities should be included.

## 3 Optimal fueling -Affine engine characteristics

It will first be assumed that engine torque can be approximated as an affine function. With inspiration from the measured data in Figure 1, the model depicted in Figure 2

Variables and parameters	Description
$\alpha$	Road slope [rad]
$\delta$	Engine fueling [kg/stroke]
$\eta$	Transmission efficiency
$\omega_e$	Engine speed [rad/s]
$\rho$	Air density [kg/m <sup>3</sup> ]
$\theta_e$	Crank shaft angle [rad]
$A$	Front area [m <sup>2</sup> ]
$c_e \delta, c_{e\omega}, c_{ec}$	Engine torque coefficients
$c_d$	Air drag coefficient
$c_{r1}, c_{r2}, c_{r3}$	Rolling resistance coefficients
$F_b$	Brake force
$g$	Gravitational acceleration
$i$	Gear ratio
$J_e$	Engine inertia [kgm]
$J_d$	Lumped driveline inertia [kgm]
$m$	Vehicle mass [kg]
$n_{cyl}$	Number of cylinders
$n_r$	Revolutions per stroke
$r$	Wheel radius [m]
$s$	Traveled distance [m]

Table 1: Variables and parameters for the truck model.

Quantity	Equation	Description
$J(i(t))$	$m + J_e i^2 \eta \frac{1}{r^2} + \frac{J_d}{r^2}$	Vehicle Inertia
$F_{air}(v(t))$	$\frac{1}{2} \rho c_d A v^2$	Air resistance
$F_{prop}(\delta(t), \omega_e(t), i(t))$	$\frac{\dot{m}}{r} (f_\delta(\delta) + f_\omega(\omega_e) + c_{ec})$	Propulsive force
$F_{roll}(v(t))$	$m(c_{r1} + c_{r2}v + c_{r3}v^2)$	Rolling resistance
$F_{slope}(\alpha(s(t)))$	$mg \sin \alpha(s)$	Force due to road slope

Table 2: Vehicle forces and inertias.

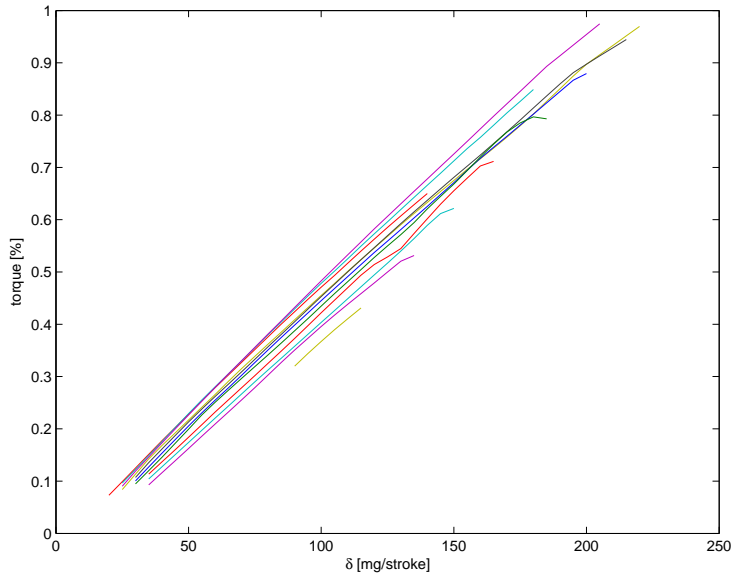


Figure 1: Measured engine torque. Each line represents a given engine speed.

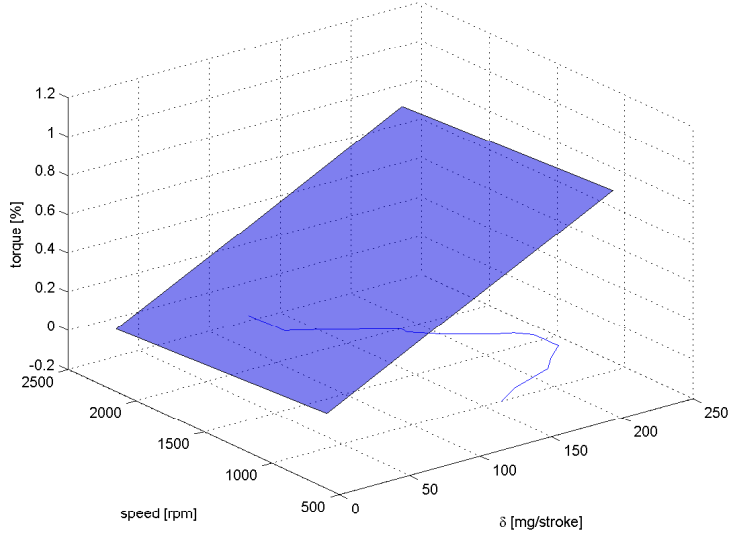


Figure 2: Affine approximation of engine torque. A maximum fueling function is also plotted as function of engine speed.

is constructed. Note that engine torque in Table 2 is  $T_e = f_\delta(\delta) + f_\omega(\omega_e) + c_{ec}$ . Using  $\omega_e = \frac{iv}{r}$ , the affine approximation of engine torque gives that  $F_{prop}$  in Table 2 is written as

$$F_{prop} = \frac{i\eta}{r} (c_{e\delta}\delta + c_{e\omega}\frac{iv}{r} + c_{ec}) \quad (4)$$

In Figure 2 the maximum fueling function for a real engine is plotted. That function will here firstly be approximated as an affine function of engine speed, but later a more exact quadratic function will be used. Again using  $\omega_e = \frac{iv}{r}$  this can be written as

$$C_\delta = \delta - (c_{\omega con}i\frac{v}{r} + c_{ccon}) \leq 0 \quad (5)$$

and it is assumed that  $\delta \geq 0$ .

Since road slope is a function of position it is convenient to change independent variable from time  $t$  to position  $s$ ,

$$\frac{d}{ds} = \frac{1}{v} \frac{d}{dt} \quad (6)$$

Let the states  $x$  of the system be vehicle speed  $v$  and traveled time  $T$ , i.e.  $x = [v, T]^T$ . Neglecting engine inertia the system dynamics becomes

$$\frac{dv}{ds} = \frac{1}{v} \left( c_\delta i \delta + c_\omega i^2 \frac{v}{r} + c_e i + c_c + c_v v + c_{v2} v^2 + c_\alpha \sin \alpha(s) \right) = f_v \quad (7)$$

$$\frac{dT}{ds} = \frac{1}{v} = f_T \quad (8)$$

where the model coefficients can be derived from those given in Tabel 1.

The fuel minimization problem will be solved with optimal control theory which is thoroughly described in the classic textbook [1], and that notation will here be followed. The function to be minimized, (1), with constraints (5), (7), (8), are used to construct the following Hamiltonian

$$H = \delta i + \lambda_v f_v + \lambda_T f_T + \mu_\delta C_\delta \quad (9)$$

where  $\frac{n_{cyl}}{2\pi n_r r}$  are included in the multipliers. When the constraint  $C_\delta$  is inactive  $\mu_\delta = 0$ , and when the constraint is active  $\mu_\delta \geq 0$ . The dynamics of the adjoint state variables are  $\frac{d\lambda}{ds} = -H_x^T$ , i.e.

$$\begin{aligned} \frac{d\lambda_v}{ds} &= \frac{\lambda_v}{v^2} (c_\delta i \delta + c_e i + c_c - c_{v2} v^2 + c_\alpha \sin \alpha) \\ &\quad + \frac{\lambda_T}{v^2} + \mu_\delta c_{\omega con} \frac{i}{r} \end{aligned} \quad (10)$$

$$\frac{d\lambda_T}{ds} = 0 \quad (11)$$

As in [11] the optimal fueling control is found by minimizing  $H$  with respect to the control variable  $\delta$ . Since the Hamiltonian is linear in  $\delta$  the optimal control sequence will consist of sections of maximum fueling, minimum fueling or sections where  $\frac{dH}{d\delta} = 0$ . The latter sections are called singular arcs. Differentiating the Hamiltonian gives

$$\frac{dH}{d\delta} = i \left( 1 + \frac{\lambda_v c_\delta}{v} \right) + \mu_\delta \quad (12)$$

For sections of singular arcs where  $C_\delta < 0$ , i.e.  $\mu_\delta = 0$ , it is seen in (12) that  $\lambda_v = -\frac{v}{c_\delta}$ . It must also hold that  $\frac{d}{ds} \left( \frac{dH}{d\delta} \right) = 0$  which gives

$$\begin{aligned} \frac{d}{ds} \left( \frac{\lambda_v c_\delta}{v} \right) &= \frac{d\lambda_v}{ds} \frac{c_\delta}{v} - \frac{\lambda_v c_\delta}{v^2} f_v \\ &= \frac{\lambda_v c_\delta}{v^3} \left( -c_\omega \frac{i^2 v}{r} - c_v v - 2c_{v2} v^2 \right) + \frac{\lambda_T c_\delta}{v^3} = 0 \end{aligned} \quad (13)$$

Putting (12) equal to zero, solving for  $\lambda_v$ , and inserting into (13) gives the following dependency between  $v$  and  $\lambda_T$

$$\frac{v^2}{c_\delta} \left( c_\omega \frac{i^2}{r} + c_v + 2c_{v2} v \right) + \lambda_T = 0 \quad (14)$$

Since  $\lambda_T$  is constant, (11), the system must be in stationarity during singular arcs, i.e.  $v$  is constant, and since (14) and  $\lambda_v = -\frac{v}{c_\delta}$ ,  $\lambda_v$  must be constant. The constant  $\lambda_T$  is determined by that the constraint on total travel time (2) is fulfilled. Given initial and end conditions on the states  $v$  and  $T$ , the complete problem to solve thus consists of Equations (2), (5), (7), (8), (10)-(12), (14).

### 3.1 Solution characteristics

As mentioned above, the optimal control sequence consists of maximum fueling, zero fueling and, singular arcs where fueling  $\delta$  is chosen such that vehicle speed is stationary. Obviously, due to the nature of the vehicle resistance forces, the global optimal solution will be stationary, i.e. constant speed, whenever it is possible, i.e. whenever

the road gradient is small enough. Road gradient is considered small if maximum fueling is enough to keep constant speed in an uphill slope and if zero fueling does not result in acceleration in a down hill slope, [2]. Such small enough gradients will here be defined. Consider the model (7) and let fueling  $\delta = 0$ . It is seen that for all inclination angles

$$\tilde{\alpha}_d \in \{\tilde{\alpha}_d : c_\omega i^2 \frac{v}{r} + c_e i + c_c + c_v v + c_{v2} v^2 + c_\alpha \sin \tilde{\alpha}_d > 0\} \quad (15)$$

the vehicle will accelerate even though the engine does not produce any work. The limit for the set  $\tilde{\alpha}_d$  is found by setting equality in (15) resulting in

$$\begin{aligned} \alpha_d &= \arcsin \frac{c_\omega i^2 \frac{v}{r} + c_e i + c_c + c_v v + c_{v2} v^2}{-c_\alpha} \\ &= \arcsin \frac{\frac{c_{e\omega} \eta i^2 v}{r^2} + \frac{c_{ec} \eta i}{r} - mc_{r1} - mc_{r2} v - mc_{r3} v^2 - \frac{1}{2} \rho c_d A v^2}{mg} \end{aligned} \quad (16)$$

that of course is a negative angle,  $\alpha_d < 0$ , for realistic vehicle parameters. For uphill slopes the vehicle will accelerate when using maximum fueling  $\delta_{max}$  for angles

$$\tilde{\alpha}_u \in \{\tilde{\alpha}_u : c_\delta i \delta_{max} + c_\omega i^2 \frac{v}{r} + c_e i + c_c + c_v v + c_{v2} v^2 + c_\alpha \sin \tilde{\alpha}_u > 0\} \quad (17)$$

and the limit for the set is

$$\begin{aligned} \alpha_u &= \arcsin \frac{c_\delta i \delta_{max} + c_\omega i^2 \frac{v}{r} + c_e i + c_c + c_v v + c_{v2} v^2}{-c_\alpha} \\ &= \arcsin \frac{\frac{c_{e\delta} \eta i}{r} \delta_{max} + \frac{c_{e\omega} \eta i^2 v}{r^2} + \frac{c_{ec} \eta i}{r} - mc_{r1} - mc_{r2} v - mc_{r3} v^2 - \frac{1}{2} \rho c_d A v^2}{mg} \end{aligned} \quad (18)$$

that is a positive angle,  $\alpha_u > 0$ .

Using Equations (16) and (18) the following definition can be made

**Definition** *Small gradients are all gradients with inclination  $\alpha$  such that*

$$\alpha_d < \alpha < \alpha_u \quad (19)$$

*Other gradients are referred to as steep gradients.*

To conclude, there are three possible control settings for optimal fueling, i.e. maximum fueling, fuel cut-off, and to control fueling such that vehicle speed is constant.

The adjoint variable  $\lambda_v$  responds to future changes in inclination  $\alpha$ , and for steep slopes maximum or minimum fueling respectively is not enough to keep  $\lambda_v$  stationary. As seen in (12)  $\frac{dH}{d\delta}$  depends on  $\lambda_v$  and hence  $\lambda_v$  is important for the control switch points. An optimal solution will thus consist of constant fueling for flat road and small gradients, but in and in a neighborhood of steep uphill slopes it will be optimal to use maximum fueling, and, in and in a neighborhood of steep downhill slopes it will be optimal to cut off the fuel injection. The importance of the adjoint variable  $\lambda_v$  will be stressed later and in Section 6.5 it will be used for a discussion on the sensitivity of the optimal solution.

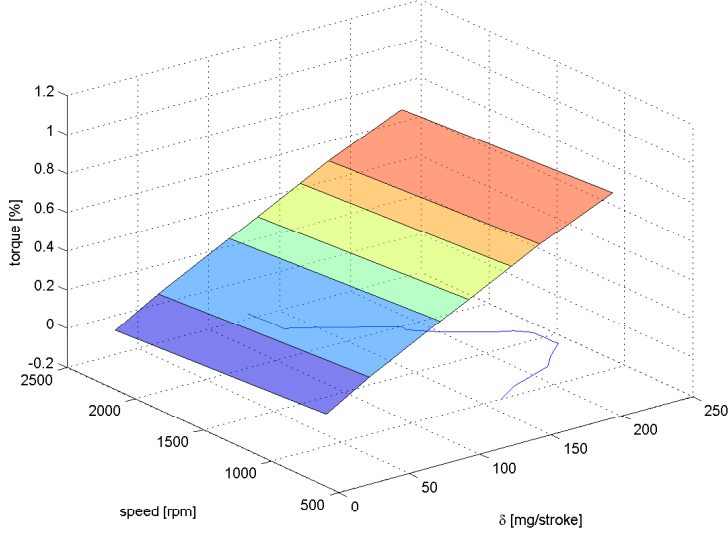


Figure 3: Engine torque as a piece-wise affine function of fueling. Maximum fueling is plotted as function of engine speed.

## 4 PWA engine characteristics

To better approximate the engine characteristics the engine torque will now be modeled as a piece-wise affine function of fueling  $\delta$ , see Figure 3 for a hypothetic example. Let fueling be divided in  $N$  regions, see Figure 4 for a schematic depiction. When the engine is operated in region  $n$  the propulsive force  $F_{prop}$  in Table 2 is written

$$F_{prop} = \frac{i\eta}{r} \left( \sum_{i=1}^{n-1} (k_{\delta,i} - k_{\delta,i+1}) \delta_{max,i} + k_{\delta,n} \delta + k_{\omega e} \omega_e + k \right) \quad (20)$$

When operating in fueling region  $n$  the vehicle dynamics can be written in the form (7) with obvious changes to the parameters, e.g. let  $c_{\delta} = c_{\delta,n} = \frac{\eta k_{\delta,n}}{Jr}$ . Differentiating the Hamiltonian with respect to fueling now gives

$$\frac{dH}{d\delta} = i \left( 1 + \frac{\lambda_v c_{\delta,n}}{v} \right) + \mu_{\delta} \quad (21)$$

Considering only the operating region where the engine is currently operating, optimal control can be derived as in Section 3, i.e. fueling can be in the limit of the region or fueling can be such that vehicle speed is constant. Each engine region can be associated with a constant speed solution as in Equation (14), i.e. the solution to

$$\frac{v^2}{c_{\delta,n}} \left( c_{\omega} \frac{i^2}{r} + c_v + 2c_{v2}v \right) + \lambda_T = 0 \quad (22)$$

For each engine operating region  $n$ , limit angles can be defined as in Equation (19) by modifying Equations (16) and (18) giving

$$\alpha_{d,n} < \alpha < \alpha_{u,n} \quad (23)$$

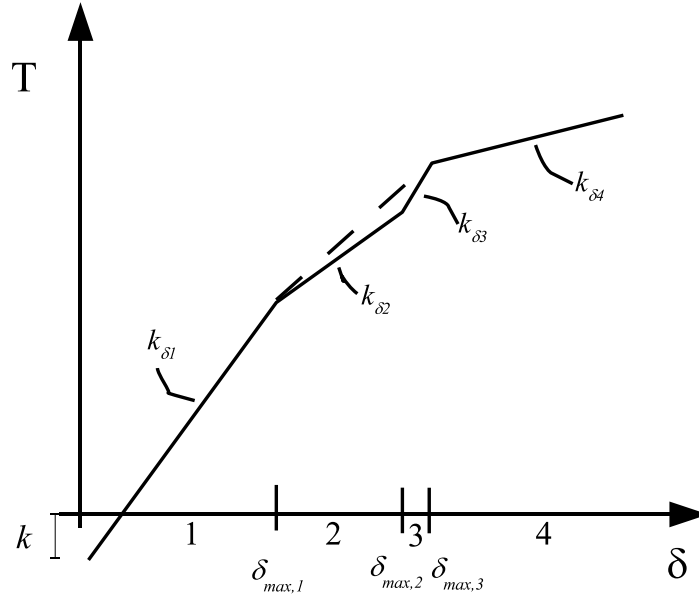


Figure 4: piece-wise affine approximation of engine characteristics.

#### 4.1 Concave engine map

Now consider a concave torque characteristic, i.e.  $c_{\delta,i} > c_{\delta,i+1}$ . From (21) it is seen that when

$$-\frac{1}{c_{\delta,i+1}} < \frac{\lambda_v}{v} < -\frac{1}{c_{\delta,i}} \quad (24)$$

it will hold that  $\frac{dH}{d\delta_i} < 0$  and  $\frac{dH}{d\delta_{i+1}} > 0$ . Since both  $v$  and  $\lambda_v$  are continuous functions the optimal control sequence will consist of a period where fueling is on the border of fueling region  $i$  and  $i+1$ . This means that there is never an immediate change from constant speed to maximum or minimum fueling, but the solution will consist of a “smoother” change to the upper or lower limit of fueling. With  $c_{\delta,i} > c_{\delta,i+1}$  the corresponding stationary solution given by (22) will be  $v_i > v_{i+1}$ . This means that some downhill slopes will have constant speed solutions with higher speed than for flat road and some uphill slopes will have constant speed solutions that is lower than for flat road.

#### 4.2 Non concave engine map

For the approximation in Figure 3 the requirement  $c_{\delta,i} > c_{\delta,i+1}$  is not fulfilled for all  $i$ , i.e. the approximation is not concave. For such a case further reasoning needs to be done in order to find the optimal control. An example fuel-torque characteristic is depicted in Figure 4. Let the torque characteristic have slope  $c_{\delta,i}$  in the respective region. Consider a case where cruising at constant speed at flat road implicates  $i = 1$ , i.e. a fueling value in region 1. When a steep uphill slope is approached there is some distance where for example  $1 + \frac{\lambda_v c_{\delta,i}}{v} > 0$  for  $i = 2, 4$  and  $1 + \frac{\lambda_v c_{\delta,i}}{v} < 0$  for  $i = 1, 3$ . For such a position, if considering only region 1 and 2 fueling would be chosen at the

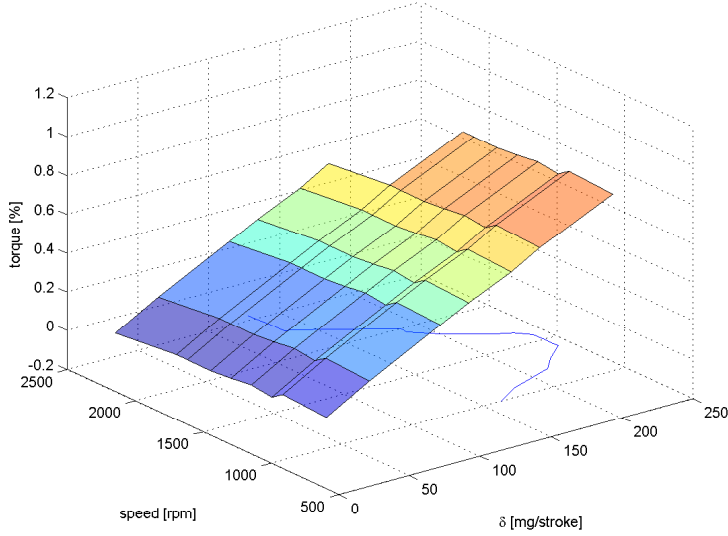


Figure 5: piece-wise affine approximation of engine characteristics. Maximum fueling is plotted as function of engine speed.

border between those regions. Considering only region 3 and 4 would in the same way give a fueling in the border between those regions. There is hence two candidate values of fueling to use. To decide which one that is optimal an approximation to the torque characteristics that reduces the number of fueling regions can be used. Such an approximation is marked as a dashed line in Figure 4. In this way the fueling-torque characteristics is transformed into a concave function and the choice of fueling is uniquely decided by considering (24). Similar reasoning can be made for downhill slopes.

### 4.3 Non linear engine speed characteristics

To further improve the approximation of the engine characteristics, non-linearities in engine speed dimension could also be considered. One way is to consider engine torque as a piece-wise affine function of both speed and fueling.

Let engine speed be divided in  $M$  regions and let fueling be divided in  $N$  regions. When the engine is operated in region  $(m, n)$  the propulsive force  $F_{prop}$  in Table 2 is written

$$F_{prop} = \frac{i\eta}{r} \left( \sum_{i=1}^{n-1} (k_{\delta,i} - k_{\delta,i+1}) \delta_{max,i} + k_{\delta,n} \delta + \sum_{j=1}^{m-1} (k_{\omega_e,j} - k_{\omega_e,j+1}) \omega_{e,max,j} + k_{\omega_e,m} \omega_e + k \right) \quad (25)$$

See Figure 5 for an hypothetical engine model with  $M = 8, N = 6$ .

Differentiating the Hamiltonian with respect to fueling gives the same result as in (21).

Considering only the operating region where the engine is currently operating, optimal control can be derived as in Section 3, i.e. fueling can be in the limit of the region or fueling can be such that vehicle speed is constant. Each engine region can be associated with a constant speed solution as in Equation (14), i.e. the solution to

$$\frac{v^2}{c_{\delta,n}}(c_{\omega,m} \frac{i^2}{r} + c_v + 2c_{v2}v) + \lambda_T = 0 \quad (26)$$

For each engine operating region  $[m, n]$ , limit angles can be defined as in Equation (19) by modifying Equations (16) and (18) giving

$$\alpha_{d,m,n} < \alpha < \alpha_{u,m,m} \quad (27)$$

Modeling engine torque as a piece-wise affine function of engine speed gives a Hamiltonian that is not differentiable with respect to  $v$ . This means that  $\lambda_v$  will have a discontinuity in the switch point between different engine speed regions. How this can be treated is described in Chapter 3.6 in [1]. However, accounting for the non-linearities in the speed dimension does not affect the principal behavior of the optimal control given by (21) in the sense that the optimal fueling also in this case is in the border of fueling regions or such that vehicle speed is constant. However, both the vehicle dynamics (7) and the adjoint dynamics (10) is affected by the engine characteristics in the speed dimension, which means that the optimal control switch points depends on it. Since the optimal fueling behavior in principal is not affected by the modeling in the speed dimension the remaining of this paper only considers nonlinearities in the fueling dimension.

A non-concave engine torque can require some care in finding the global optimal solution. One such case is treated in [8]. That case is when the desired average speed corresponds to an inefficient engine operating point. Then it can be optimal to switch between two other cruising speeds resulting in correct average speed. This can be studied using Equation (26). For a given  $\lambda_T$  it can be the case that no region has a feasible constant speed solution corresponding to desired average speed. In such a case the optimal solution consists of switching between different cruising speeds.

Other ways than (25) to make a PWA approximation of the engine map can be more close to the real characteristics. For example one can use a triangular mesh or a bilinear function of engine speed and fueling. However, such approximations would still keep the problem in input affine form and the principal results discussed so far would not be changed.

## 5 Optimal gear ratio control

Not only fueling control but also gear choice affects the fuel consumption considerably. Although there are high-power applications for which continuously variable transmissions are used [14, 17], the most common transmission for heavy trucks are the discrete step transmission. As a first attempt to study fuel optimal gear shifting, gear ratio  $i$  is assumed to be continuously variable and fulfilling  $0 < i_{min} \leq i \leq i_{max}$ . Later, those results will be used to derive solutions for a stepped transmission.

### 5.1 Optimal gear ratio - affine maximum fueling

Again study the model with affine engine characteristics (4) from Section 3. Maximum fueling will here be modeled as an affine function of engine speed by using  $\omega_e =$

$\frac{iv}{r}$  in (5). Although this is a too simple model to resemble the measured function in Figure 2 the results are illustrative and a base for the more accurate quadratic model that will be used in Section 5.2.

The gear ratio can be varied between a lower and upper limit, i.e., it has to fulfill the following constraints

$$C_{imax} = i - i_{max} \leq 0 \quad (28)$$

$$C_{imin} = i_{min} - i \leq 0 \quad (29)$$

When choosing gear ratio the engine speed must also be kept within limits, i.e.

$$C_{\omega min} = \omega_{min} - \frac{iv}{r} \leq 0 \quad (30)$$

$$C_{\omega max} = \frac{iv}{r} - \omega_{max} \leq 0 \quad (31)$$

The constraints (28)-(31) are adjoined to the Hamiltonian with respective Lagrange multipliers  $\mu_{imax}$ ,  $\mu_{imin}$ ,  $\mu_{\omega min}$ , and  $\mu_{\omega max}$ .

$$H = \delta i + \lambda_v f_v + \lambda_T f_T + \mu_\delta C_\delta + \mu_{imax} C_{imax} + \mu_{imin} C_{imin} + \mu_{\omega min} C_{\omega min} + \mu_{\omega max} C_{\omega max} \quad (32)$$

Differentiating the Hamiltonian (32) with respect to  $i$  gives

$$\frac{dH}{di} = \delta \left(1 + \frac{\lambda_v c_\delta}{v}\right) + 2c_\omega \frac{\lambda_v}{r} i + c_e \frac{\lambda_v}{v} - \mu_\delta c_{\omega con} \frac{v}{r} + \mu_{imax} - \mu_{imin} - \mu_{\omega min} \frac{v}{r} + \mu_{\omega max} \frac{v}{r} \quad (33)$$

During sections of constant speed, i.e. for flat road and small gradients, fueling is not in the limit, i.e.  $\mu_\delta = 0$ . Then Equation (12) gives  $1 + \frac{\lambda_v c_\delta}{v} = 0$ . Also assume that gear ratio and engine speed is within allowed limits, i.e. the respective  $\mu = 0$ . The condition  $\frac{dH}{di} = 0$  then gives the optimal gear ratio

$$i_{opt} = -\frac{c_e}{c_\omega} \frac{r}{2v} \quad (34)$$

For typical engine characteristics, see Figure 1,  $c_e, c_\omega < 0$  or  $c_\omega < 0$  and  $c_e$  is small. Both situations result in that  $i_{opt}$  given by (34) is smaller than  $i_{min}$ , and hence, considering limits on  $i$  the resulting optimal solution is  $i_{opt} = i_{min}$ . This minimizes engine speed and hence engine friction.

Assuming that engine speed limits and gear ratio limits are not reached, i.e.  $\mu_{\omega min} = \mu_{\omega max} = \mu_{imin} = \mu_{imax} = 0$ , optimal gear ratio during sections of maximum fueling is found by combining Equations (5), (12), and, (33), using  $\frac{dH}{d\delta} = \frac{dH}{di} = 0$ , which gives

$$\begin{aligned} \frac{dH}{di} &= c_{con} \left(1 + \frac{\lambda_v c_\delta}{v}\right) + c_e \frac{\lambda_v}{v} \\ &+ \frac{2}{r} (c_{\omega con} v \left(1 + \frac{\lambda_v c_\delta}{v}\right) + c_\omega \lambda_v) i = 0 \end{aligned} \quad (35)$$

The optimal gear ratio given by Equation (35) is

$$i_{opt} = -\frac{c_{con} \left(1 + \frac{\lambda_v c_\delta}{v}\right) + c_e \frac{\lambda_v}{v}}{\frac{2}{r} (c_{\omega con} v \left(1 + \frac{\lambda_v c_\delta}{v}\right) + c_\omega \lambda_v)} \quad (36)$$

Recall that  $1 + \frac{\lambda_v c_\delta}{v} < 0$  during sections where maximum fueling is used. It will be shown later in simulations that  $1 + \frac{\lambda_v c_\delta}{v}$  gets a large magnitude in steep uphill slopes resulting in high gear ratios. Before and after the slope a low gear is used as given by (34). For the model considered  $c_{con} c_\delta$  is about 7 times  $c_e$ , giving high gear ratios in steep uphill slopes. However, large magnitudes on  $c_{\omega con}$  limits the gear ratio to a lower gear ratio.

## 5.2 Optimal gear ratio - quadratic maximum fueling

To make a better approximation of maximum fueling than (5) the following quadratic model is used

$$C_\delta = \delta - (a_0 + a_1 \frac{iv}{r} + a_2 (\frac{iv}{r})^2) \leq 0 \quad (37)$$

Another choice could be to make a piece-wise affine model, but then the Hamiltonian will not be differentiable with respect to vehicle speed.

The optimal gear ratio is now given from

$$\begin{aligned} \frac{dH}{di} = \delta \left(1 + \frac{\lambda_v c_\delta}{v}\right) + 2c_\omega \frac{\lambda_v}{r} i + c_e \frac{\lambda_v}{v} - \mu_\delta \left(a_1 + 2a_2 \frac{iv}{r}\right) \frac{v}{r} + \mu_{imax} - \mu_{imin} \\ - \mu_{\omega min} \frac{v}{r} + \mu_{\omega max} \frac{v}{r} = 0 \end{aligned} \quad (38)$$

When using maximum fueling and assuming that gear ratio limits as well as engine speed limits are not reached, optimal gear ratio is found by combining Equations (12), (37), and (38), which gives

$$\begin{aligned} 3a_2 \frac{v^2}{r^2} \left(1 + \frac{\lambda_v c_\delta}{v}\right) i^2 + \left(2a_1 \frac{v}{r} \left(1 + \frac{\lambda_v c_\delta}{v}\right) + 2c_\omega \frac{\lambda_v}{r}\right) i + a_0 \left(1 + \frac{\lambda_v c_\delta}{v}\right) + c_e \frac{\lambda_v}{v} \\ = k_2 i^2 + k_1 i + k_o = 0 \end{aligned} \quad (39)$$

Now the optimal gear ratio is

$$i_{opt} = -\frac{k_1}{2k_2} \pm \sqrt{\left(\frac{k_1}{2k_2}\right)^2 - \frac{k_o}{k_2}} \quad (40)$$

Typically, only the solution with the plus sign before the square root gives physically feasible solutions.

**Plots of optimal gear solutions.** In Figure 6 the solution to Equation (39) is plotted as a function of the decisive variable  $1 + \frac{\lambda_v c_\delta}{v}$  and vehicle speed  $v$ . The lowest possible gear ratio for the vehicle studied is 3.42. Recall that during sections of constant speed  $1 + \frac{\lambda_v c_\delta}{v} = 0$ . Consider the case where cruising speed is 85 km/h and the vehicle is approaching a steep uphill slope. During acceleration before the slope speed will increase and the term  $1 + \frac{\lambda_v c_\delta}{v}$  will decrease, i.e. the operating point will move downwards to the right in Figure 6. One conclusion that can be drawn from this figure is that it will never be optimal to change gear during the acceleration phase before a steep uphill slope. When the vehicle starts to climb the hill speed will decrease, shifting the operating point to the left, and the operating point enters the region for a possible gear change.

Another thing to notice in Figure 6 is that for large magnitudes of  $1 + \frac{\lambda_v c_\delta}{v}$  the optimal gear ratio is approximately a function of vehicle speed since the gear ratio contours

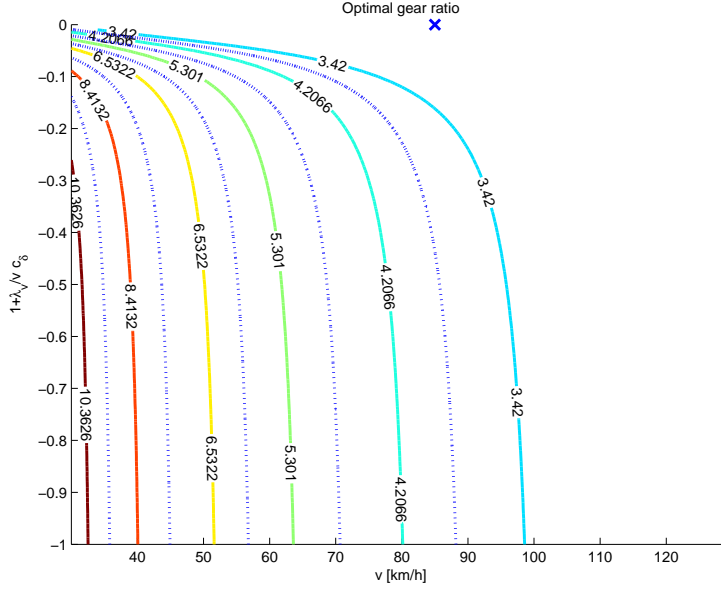


Figure 6: Contour plot of the optimal gear ratio,  $i$ , given by Equation (39). The operating point for stationary vehicle speed at 85 km/h is marked by a cross. The contours are drawn at gear ratio levels corresponding to a discrete step transmission. The dashed lines are the optimal gear shifting points for a discrete step transmission.

are almost vertical. As will be shown later in simulations that region is reached when maximum fueling has been used for a longer period of time, i.e. for relatively long or steep uphill slopes.

For any given vehicle speed it is equivalent to see engine speed  $\omega_e$  as control variable instead of gear ratio  $i$  using  $\omega_e = \frac{v}{r}$ . Using this substitution in Equation (39) optimal engine speed can be calculated and a contour plot of the achieved result is plotted in Figure 7. It can be seen in the area to the left of the dotted line in Figure 7 that optimal engine speed very well can be described as a function of the decisive variable  $1 + \frac{\lambda_v c_\delta}{v}$ , since the lines are almost horizontal. To the right of the dotted line the solution is restricted by the minimum allowed gear ratio, compare with Figure 6. As will be shown later in simulations the magnitude of the decisive expression  $1 + \frac{\lambda_v c_\delta}{v}$  depends highly on the length and inclination of uphill slopes. A longer or steeper slope results in larger magnitude of  $1 + \frac{\lambda_v c_\delta}{v}$ , which means that optimal engine speed is a function of length and steepness of the slope.

**Further analysis and implications of optimality.** If the quadratic maximum fueling function is linearized it can be compared with the result in (36). The linearization of the quadratic model in the point  $\omega_0$  is

$$C_\delta = \delta - (a_0 - a_2 \omega_0^2 + (a_1 + 2a_2 \omega_0) \omega) \leq 0 \quad (41)$$

Considering (36) and assuming that  $1 + \frac{\lambda_v c_\delta}{v}$  has a large magnitude,  $i_{opt}$  can be approximated as

$$i_{opt} = -\frac{c_{con}}{2 C_{\omega con} v} \quad (42)$$

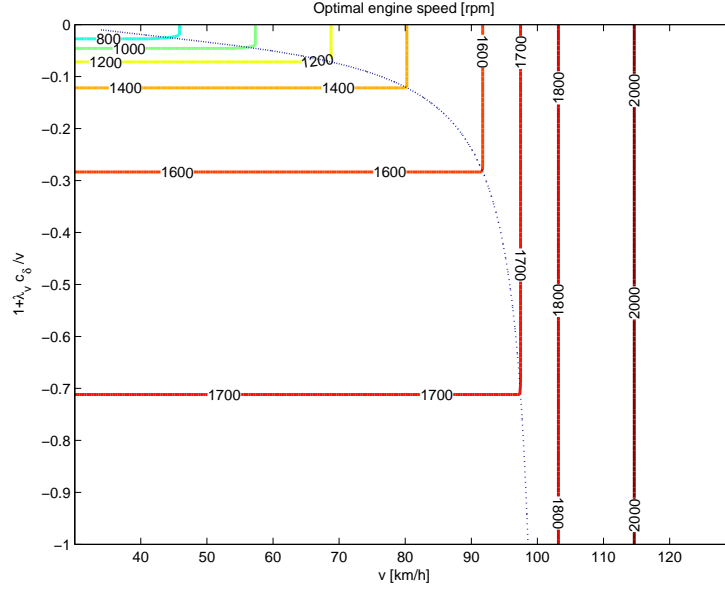


Figure 7: Contour plot of optimal engine speed.

Again using engine speed as an equivalent control instead of gear ratio, using the substitution  $\omega_e = \frac{v_i}{r}$ , an optimal engine speed can be calculated for every vehicle speed. Rewriting (42) to optimal engine speed gives

$$\omega_{opt} = -\frac{c_{con}}{2c_{\omega con}} = -\frac{a_0 - a_2\omega_0^2}{2(a_1 + 2a_2\omega_0)} \quad (43)$$

There is one engine speed  $\omega_0 = \omega^*$  where  $\omega^* = -\frac{a_0 - a_2\omega^{*2}}{2(a_1 + 2a_2\omega^*)}$ . For  $\omega_0 < \omega^*$  it holds that  $\omega_{opt} > \omega^*$  and for  $\omega_0 > \omega^*$  it holds that  $\omega_{opt} < \omega^*$ . Hence it is never beneficial to operate at a higher engine speed than  $\omega^*$ . Rewriting (43) the optimal engine speed is found by solving the following equation

$$3a_2\omega_{opt}^2 + 2a_1\omega_{opt} + a_0 = 0 \quad (44)$$

Using  $\omega_e = \frac{v_i}{r}$  this expression is quite similar to (39). It will now be shown that when  $\left|\frac{\lambda_v c_{\delta}}{v}\right| \gg 1$ , optimal engine speed goes to the same engine speed as where maximum torque to the wheels are delivered. The torque delivered by the engine to the wheels is

$$T_w = \frac{r\omega_e}{v}\eta T_e = \frac{r\omega_e}{v}\eta(c_{e\delta}(a_0 + a_1\omega_e + a_2\omega_e^2) + c_{e\omega}\omega_e + c_{ec}) \quad (45)$$

This equation is differentiated with respect to  $\omega_e$  to find the engine speed that gives maximum torque to the wheels. This is also the engine speed where the engine produces maximum power.

$$\frac{dT_w}{d\omega_e} = \frac{r\eta}{v}(c_{e\delta}(a_0 + 2a_1\omega_e + 3a_2\omega_e^2) + 2c_{e\omega}\omega_e + c_{ec}) = 0 \quad (46)$$

Consider Equation (39), notice that when  $\left|\frac{\lambda_v c_{\delta}}{v}\right| \gg 1$ , the optimal engine speed goes to the solution of Equation (46). Also, since  $|c_{e\delta}| \gg |c_{e\omega}|, |c_{ec}|$ , this solution is close

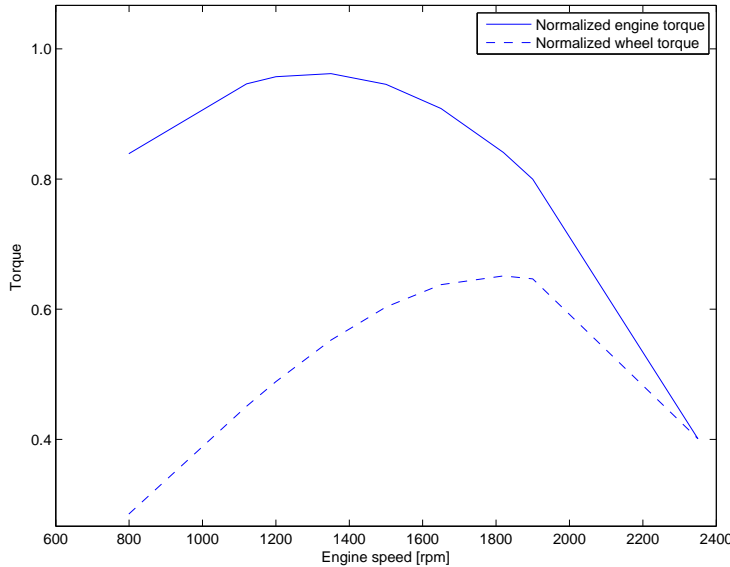


Figure 8: Maximum engine torque and maximum wheel torque. At about 1800 rpm the engine delivers maximum torque to the wheels.

to the solution of Equation (44). For the engine considered and the quadratic maximum fueling function, maximum engine torque and maximum wheel torque (maximum engine power) are plotted in Figure 8. The conclusion from this is that the character of the maximum fueling function is decisive for the optimal gear choice.

### 5.3 Discrete step transmission

Since discrete step transmissions are the most commonly used transmission for heavy trucks it is interesting to see how the optimal solution would be if the gear ratio belongs to a set of discrete numbers  $i \in \{i_1, i_2, \dots, i_n\}$ . For this case Equation (33) can no longer be used directly to find the optimal gear ratio.

As a first attempt to model the gear shift process it will be assumed that a gear shift is carried out instantaneously but possibly with a discontinuity in vehicle speed. For vehicles with mechanical solutions such as for example dual clutch transmissions there is no disruption in torque during a gear shift, and hence it is feasible to model the gear shifting without any speed loss. Using the more common manual transmissions there is a disruption in torque, and such gear shifts will, except in steep downhills, result in a decrease in speed. Suppose that a gear shift occurs at position  $s = s_i$  for a set of gear shifting positions  $s_i \in \{s_1, \dots, s_{N-1}\}$ , and let the speed just before the shift be  $v(s_{i-})$ , let the speed just after the shift be  $v(s_{i+})$ , and let the decrease in speed during the shift be  $v_s$ . The shift is then modeled as

$$v(s_{i-}) - v(s_{i+}) = v_s \quad (47)$$

One way to handle the discontinuity in this problem is to consider both fueling and gear choice as control variables. The optimal control is then found by searching for the control that minimizes the Hamiltonian at every position, see the discussion on the maximum principle in [11]. Another approach that will be used here is described in [1].

Then only fueling is considered as a control variable that is found from  $\partial H/\partial u = 0$ . This leads to a formulation with switching between different system dynamics functions when switching gear. The optimal control problem formulation with discontinuities in the system equations and in the state variables, as described in Chapter 3.7 in [1] is used here. The gear shifting function

$$\phi = v(s_{i-}) - v(s_{i+}) - v_s = 0 \quad (48)$$

is adjoined to the performance criteria with multiplier  $\vartheta$ . Let

$$\phi = \vartheta\phi \quad (49)$$

and the Hamiltonian be the combination of the Hamiltonians for each interval

$$H^{(i)} = L^{(i)} + \lambda^T f^{(i)} \quad (50)$$

For  $N - 1$  shifts the performance criteria is

$$J = \sum_{j=1}^{N-1} \vartheta^{(j)T} \phi^{(j)} + \sum_{i=1}^N \int_{s_{i-1}^+}^{s_i^-} (L^{(i)} + \lambda^T f^{(i)} - \lambda^T \frac{dx}{ds}) ds \quad (51)$$

It is shown in [1] that necessary conditions for optimality is

$$\frac{d\lambda}{ds} = - \left( \frac{\partial H^{(i)}}{\partial x} \right)^T, \quad s_{i-1}^+ < s < s_i^- \quad (52)$$

$$\lambda^T(s_{i-}) = \frac{\partial \phi}{\partial x(s_{i-})} \quad (53)$$

$$\lambda^T(s_{i+}) = - \frac{\partial \phi}{\partial x(s_{i+})} \quad (54)$$

$$H^{(i)}(s_{i-}) - H^{(i+1)}(s_{i+}) = 0 \quad (55)$$

For the case (48)  $\lambda_v(s_{i-}) = \lambda_v(s_{i+}) = \vartheta_i$ , i.e. the adjoint variable  $\lambda_v$  is continuous over a gear shift.

Since  $\lambda_v$  is continuous and gear ratio should be chosen such that the Hamiltonian is minimized at each position, a change in gear can only occur when the Hamiltonian evaluated for two nearby gears equal each other, i.e.  $H(i_i, v(s_{i-})) = H(i_{i+1}, v(s_{i+}))$ . For zero speed loss at shifting points, i.e.  $v_s = 0$ , the resulting gear shifting points are marked with dashed lines in Figure 6. The optimal solution with a stepped transmission will of course be quite similar to the continuously variable ratio solution in the sense that the gear ratio is chosen such that the engine speed is on average close to the continuous case. See Figure 9 for a depiction of typical gear shifting points when the speed loss of a gear shift is set to 0.1 m/s.

#### 5.4 Optimal gear ratio for PWA engine characteristics

For non-linear engine characteristics it is interesting to study gear choice also when fueling is not in the limit. For a PWA model as (25) each engine region can be analyzed separately as in Section 5.1. During constant speed sections each region  $\{m, n\}$  has an optimal gear ratio as in (34)

$$i_{opt} = - \frac{c_{e,m,n}}{c_{\omega,m}} \frac{r}{2v} \quad (56)$$

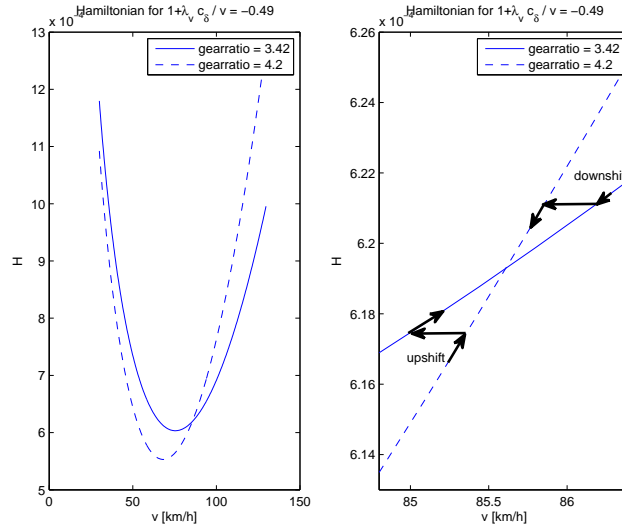


Figure 9: To the left, the Hamiltonian evaluated for a fixed ratio of  $\lambda_v/v$  and for the two highest gears. To the right, a zoom in of the left plot. The arrows indicates where downshift and upshift occurs when the speed loss of a gear shift is set to 0.1 m/s

In most cases the optimal gear ratio for each region is such that the engine speed is in the border of the regions. This means that there are some operating points that have to be considered and the optimal gear ratio is chosen such that engine efficiency is maximized. Again, if searching for optimal gear ratio during non stationary sections the engine torque has to be modeled such that the Hamiltonian is differentiable with respect to speed.

## 6 Simulations

The results from previous sections will now be demonstrated in simulations of some constructed road profiles. Both affine and piece wise affine engine models will be used, but all simulations will use the quadratic maximum fueling function (37). Also results from both continuous variable transmission as well as discrete stepped transmission will be presented. The road profiles will consist of flat road followed by an uphill slope or a downhill slope of constant gradient, and then flat road again. For such road segments the slope  $\alpha$  will have a discontinuity when changing from flat road to slope. If there is such a discontinuity at a given position  $s_d$  it is according to theory possible that the Hamiltonian and/or the adjoint variables have a discontinuity at that position. For simulation it is important to decide whether or not the adjoint variables have discontinuities, and it will here be shown that that is not the case. A general condition that decides at which position  $s_1$  such an event occurs can be formulated as in [1] as a so called interior boundary condition

$$N(x(s_1), s_1) = 0 \quad (57)$$

In Chapter 3.5 in [1] the influence on  $H$  and  $\lambda$  from such an event is derived to be

$$\lambda^T(s_{1-}) = \lambda^T(s_{1+}) + \pi^T \frac{\partial N}{\partial x(s_1)} \quad (58)$$

$$H(s_{1-}) = H(s_{1+}) - \pi^T \frac{\partial N}{\partial s_1} \quad (59)$$

where  $\pi$  are constant multipliers. Since road slope is a function of position the condition that decides when a discontinuity in  $\alpha$  occurs can be formulated as

$$N(s) = s_1 - s = 0 \quad (60)$$

For the condition (60) it is seen from (58) that there is no discontinuity in the adjoint variables  $\lambda$  since the condition is independent of the states.

## 6.1 Optimal solutions for uphill and downhill slopes

Optimal solutions of example simulations are seen in Figures 10, 11 and, 12. All simulations are of a 40 ton truck with  $\lambda_T$  chosen such that cruising speed at flat road is 85 km/h. In Figure 10 the engine model is piece-wise affine in fueling dimension and affine in speed dimension, see Figure 3. Assuming a continuously variable transmission both fueling and gear ratio is optimized. As expected from Section 5.2 and especially Equations (39) and (46), for long steep slopes the gear ratio is chosen such that the engine speed is close to 1800 rpm, the point of engine maximum power. Also as mentioned in Section 5.2 in connection to Figure 6, starting at 85 km/h before the slope there is no change in gear ratio during the acceleration phase before the slope. Notice also that the acceleration from about position 300 m to 2400 m is done using fueling in the border between the two upper fueling regions. Then, between about 2400 m to 5200 m maximum fueling is used, and from 5200 m to 6900 m fueling is again in the border between the two upper fueling regions.

In Figure 11 a simulation of the PWA engine model is done in a 500 m slope of  $-6\%$  slope. The vehicle cruises at constant speed from start to about 800 m where the fueling is lowered to the border between fueling region 2 and 3. During that part it begins to decelerate and at about 2400 m the fuel injection is again lowered to the border between region 1 and 2. It is worth noting that the fuel injection is never cut off totally as it would have been done for an affine engine torque model.

## 6.2 Affine and piece-wise affine modeling

In Figure 12 three simulations are presented. The solid line is a simulation of the affine engine torque model with no gear optimization. The dashed line is with the PWA engine torque model with no gear optimization. The dotted line is also with the PWA model but now with gear optimization. As expected the affine model only uses two modes of fueling, i.e. such that constant speed is kept to about 2300 m, and then maximum fueling is used until 5300 m where speed is kept constant again. The simulation with the PWA model start accelerating earlier and uses only maximum fueling from about 3900 m to about 4200 m. The gradual change in fueling for the PWA model gives a smoother control but also requires about 500 m longer prediction horizon than the affine model. When also gear ratio is optimized the PWA model never uses maximum fueling.

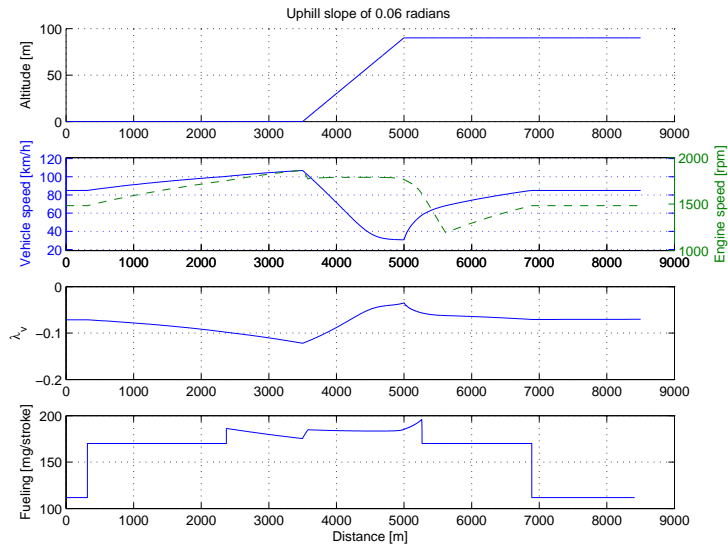


Figure 10: Uphill slope of 1500 m 6 percent inclination. Both fueling and gear ratio is optimized.

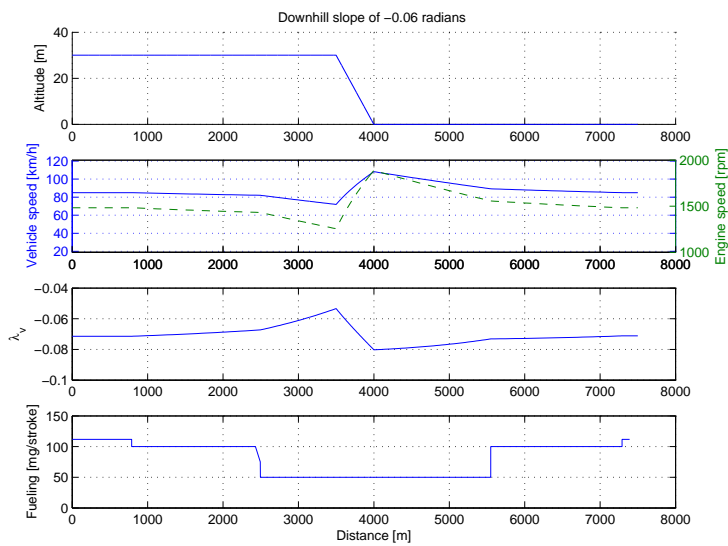


Figure 11: Downhill slope of 500 m -6 percent inclination. Both fueling and gear ratio is optimized.

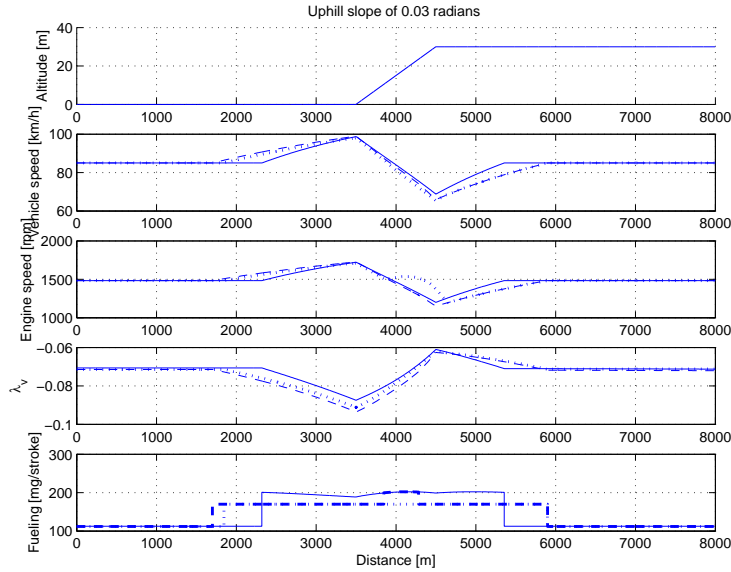


Figure 12: Three simulations in a 1000 m 3 percent uphill slope. Solid line is an affine engine torque model. Dashed line is PWA engine torque model. Dotted line is PWA engine torque model with gear optimization.

### 6.3 Continuously variable gear ratio optimization

To study optimal choice of gear ratio three simulations of the affine engine torque model is presented in Figure 13. The optimal engine speed given by Equation (39) for the three simulations are there shown as functions of vehicle speed and the decisive variable  $1 + \frac{\lambda_v c_s}{v}$ . One simulation, the “inner arc”, is of a 1000 m 3 % uphill slope. In that simulation the optimal gear ratio just about reaches the lowest feasible gear ratio. The other simulations is of a 600 m 6 % uphill slope and a 1500 m 6 % uphill slope. In the latter simulation the vehicle is able to keep a constant speed of about 30 km/h at some part of the slope. As mentioned earlier the magnitude of  $1 + \frac{\lambda_v c_s}{v}$  gets larger the longer and steeper the slope is. Hence, optimal engine speed is a function of length and steepness of the slope.

In Figure 14 the same simulation as in Figure 10 with the PWA modeled engine is depicted. Only the part in the upper fueling region is shown. Note that the optimal engine speed, being around the line 1780 rpm, is higher than for the affine engine, Figure 13, where it was around 1650 rpm, and closer to maximum engine power, Figure 8 where the maximum is around 1800 rpm.

The result from Figures 6 and 7 could be used to define gear shifting points that is dependent on speed and for example length and slope of hills. If the vehicle is approaching a long and or steep slope the magnitude of  $1 + \frac{\lambda_v c_s}{v}$  will get larger leading to a higher optimal engine speed during the slope. Looking at the simulations in for example Figure 13 it is seen that during the uphill slope, the retardation phase, the optimal engine speed has small variations with a mean value depending on the speed at the start of the slope. Hence, an approximative gear shifting strategy could be designed based on the speed when starting to climb a hill.



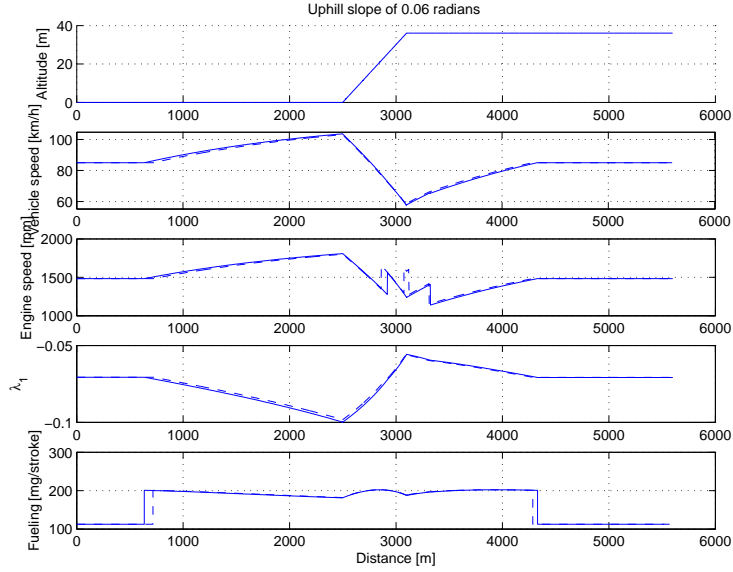


Figure 15: Simulations with an affine engine and stepped transmission in a 6% 600 m uphill slope. The engine speed is on average close to the continuous ratio solution in Figure 13. Dashed line corresponds to a simulation without a speed loss during the gear shifts, and solid line corresponds to a simulation with 0.1 m/s speed loss during the gear shifts. Note that without gear shift losses an extra gear shift occurs near the top of the hill.

#### 6.4 Discrete stepped transmission

Last, two simulations of a stepped transmission is presented. See Figure 15 for example simulations in a 6% 600 m uphill slope. The dashed lines in the figure corresponds to a simulation without a speed loss during the gear shifts, and the solid lines corresponds to a 0.1 m/s speed loss during shifts. This is a typical value if it is assumed that the engine is incapable to propel the vehicle for about 0.5 s during the shift. Note that the simulation without gear shifting losses performs an extra gear shift near the top of the hill. Note also that the engine speed is on average close to the continuous ratio solution in Figure 13.

#### 6.5 Interpretation of the Lagrange variables

Looking at the Hamiltonian (9), it is seen that it is proportional to amount of fuel used per distance, i.e. [kg/m]. This means that the Lagrange variable  $\lambda_v$  is proportional to amount of fuel divided by velocity, i.e. [kg/(m/s)]. Since  $\lambda_v$  is decisive for the optimal control it is interesting to interpret the value of it. In [1] it is shown that for the augmented performance criteria  $\bar{J} = \int_{s_0}^{s_f} (\delta i + \lambda^T (f - \frac{dx}{ds})) ds$ , the variation in the performance criteria  $\delta \bar{J}$  due to a variation in initial conditions  $\delta x(s_0)$  is

$$\delta \bar{J} = \lambda^T(s_0) \delta x(s_0) + \int_{s_0}^{s_f} \frac{\partial H}{\partial u} \delta u ds \quad (61)$$

where  $u$  is the control vector  $[\delta i]^T$ . Hence,  $\lambda^T(s_0)$  is the gradient of  $\bar{J}$  with respect to initial conditions while holding  $u(s)$  constant. Of course the position  $s_0$  can be taken

anywhere which means that  $\lambda$  at every position is a measure of how much the total cost would be affected by a change in  $x$  at that position. The variable  $\lambda_v$  thus is a measure of how much fuel consumption would change if the speed  $v$  is varied. Since  $\lambda_v$  is negative a raise in vehicle speed by 1 m/s at position  $s_0$  will result in a decreased total cost given by the value of  $\lambda_v(s_0)$ . A decrease of speed by 1 m/s would increase the total cost by the same amount.

Now, looking at the simulations above in for example Figures 10 and 11, it is seen that for an uphill slope a change in speed in the beginning of the slope has the highest influence on the total consumption. In the same way the speed at the end of a down hill slope is most critical to the total fuel consumption.

The influence from a change in vehicle speed on the total cost,  $\lambda_v(s_0)\delta v(s_0)$ , can be written as

$$\frac{\lambda_v(s_0)}{v(s_0)} v(s_0) \delta v(s_0) \quad (62)$$

Remember that the term  $\lambda_v/v$  is decisive for both optimal fueling and for optimal gear ratio. Rewriting (61) the first part is (62). Since  $v\delta v$  is a measure of change in kinetic energy,  $\lambda_v/v$  is a measure of how the total cost is affected to a change in kinetic energy. Looking at Figure 13 it is seen that the point most sensitive to a change in kinetic energy does not coincide with the point most sensitive to a change in vehicle speed. Instead of the beginning of the slope now a point somewhere in the middle of the slope is most critical, i.e. the lowest point of the respective arc. However, as mentioned earlier, the decisive factor  $1 + \frac{\lambda_v c_\delta}{v}$  has small variations during the slope which means that the sensitivity to a change in kinetic energy is approximately constant during the slope.

## 6.6 Speed limits

Speed limits is a state variable inequality constraint. Optimal control with such constraints are treated in Section 3.11 in [1]. An upper speed limit is derived by the following constraint

$$C_v = v - V_{max} \leq 0 \quad (63)$$

In [1] the method to handle the type of constraint as (63) are to differentiate until the control variable appears explicitly. For the model (7) this means that the derivative  $C'_v = \frac{d}{ds} C_v$  is adjoined to the Hamiltonian (9) with the multiplier  $\mu_v$  resulting in

$$H = \delta i + (\lambda_v + \mu_v) f_v + \lambda_T f_T + \mu_\delta C_\delta \quad (64)$$

At the entry point of a constrained arc the adjoint variable  $\lambda_v$  is discontinuous but continuous at the exit point. However, instead of solving the optimal control problem as before the constrained solution can intuitively be found from the unconstrained solution. Consider the cases presented so far. If there had been an upper speed constraint present the solution after the position of leaving the constrained arc would follow the unconstrained solution. For example, after a steep downhill slope where the unconstrained solution exceeds the speed limit at the end of the slope, the constrained solution could be found in the same way as before, by setting the speed at the end of the slope to the maximum allowed speed. The value of  $\lambda_v$  is then given by the fact that both  $\lambda_v$  and  $v$  should reach their respective stationary values at the same position. Since  $\lambda_v$  has a discontinuity at the entry point of the constrained arc there is no easy way to decide the value of  $\lambda_v$  at that point. However, among all solutions that fulfills the necessary conditions for optimality, (10)-(13), the most fuel efficient solution is to start

to decelerate before the slope at a position such that the upper speed limit is reached exactly at the end of the slope. This is of course then the solution that minimizes brake usage, and hence minimizes the total fuel consumption.

For uphill slopes the reasoning can be done in the same way such that maximum allowed speed is reached exactly at the beginning of the slope if the unconstrained solution exceeds the speed limit at that position. An example simulation with an affine engine torque model is plotted in Figure 16 where the maximum allowed speed was 90 km/h. If Figure 16 is compared to an unconstrained simulation of the same slope in Figure 13 it is seen that in the constrained simulation the optimal gear ratio in the slope is higher resulting in about 100 rpm higher engine speed than in the unconstrained case.

## 6.7 Discussion

The optimal strategies presented above is a compromise between running the engine at efficient operating points and minimizing air and roll resistance. For the affine engine model (4) the optimal fueling strategy has the character of bang-bang control. This strategy minimizes vehicle speed variations and hence air and roll resistance losses. When using the non linear model (20) the engine efficiency decreases in the upper fueling region. Hence the optimal solution in for example Figure 12 starts to accelerate earlier than when using an affine model. Using this strategy, vehicle losses for the driving mission is increased but the distance of maximum fueling, where engine efficiency is low, is shortened. Looking in the same figure it is also seen that, by optimizing gear ratio, the upper fueling region is avoided, though the higher gear ratio gives increased engine friction.

## 7 Sensitivity analysis

For an implementation in a vehicle it is interesting to see how uncertainties in parameters will affect the optimal strategy and thereby the total fuel consumption. Using a given fueling strategy and gear choice, an error in a parameter estimation will result in a different speed profile than predicted. To see how much such a change will affect the total cost the discussion in Section 6.5 can be used. As mentioned,  $\lambda_v$  is a measure of how much the total fuel consumption is affected by a change in vehicle speed. Thus, to estimate how a parameter change influences the total fuel consumption it is sufficient to study how a parameter change affects vehicle speed. The sensitivity of a function  $f(x)$  to  $x$  at the point  $x_0$  is computed as  $(\partial f/\partial x)|_{x_0}/(x_0/f(x_0))$ . In Table 3 the sensitivity of the vehicle dynamics, i.e. the right hand side of Equation (7), to the model coefficients, is presented. Road slope has the highest significance on the total fuel consumption. The second highest influence has  $c_\delta$ , and the third highest influence has  $c_c$  and  $c_{v2}$ . Note that if the drive line inertias  $J_e$  and  $J_d$  are neglected in the total vehicle inertia, see Table 2,  $c_\delta = (i\eta c_{e\delta})/(mr)$ ,  $c_{v2} = (0.5\rho c_d A + mc_{r3})/m$ ,  $c_c = (i\eta c_{ec} + mc_{r1})/m$ , and  $c_\alpha = g$ . This means for example that a fault in vehicle mass or fuel-torque characteristic has equal importance. However, a fault in road slope has the most significant influence on the total cost.

One parameter known to be difficult to measure is vehicle mass and therefore it is of special interest to study. To see how a fault in vehicle mass affects the optimal solution two simulations has been performed with masses 40 tons and 44 tons, see Figure 17. It is there seen that if the vehicle mass is underestimated, the vehicle will start to accelerate too late and shift to lower gear too late which can lead to a necessary

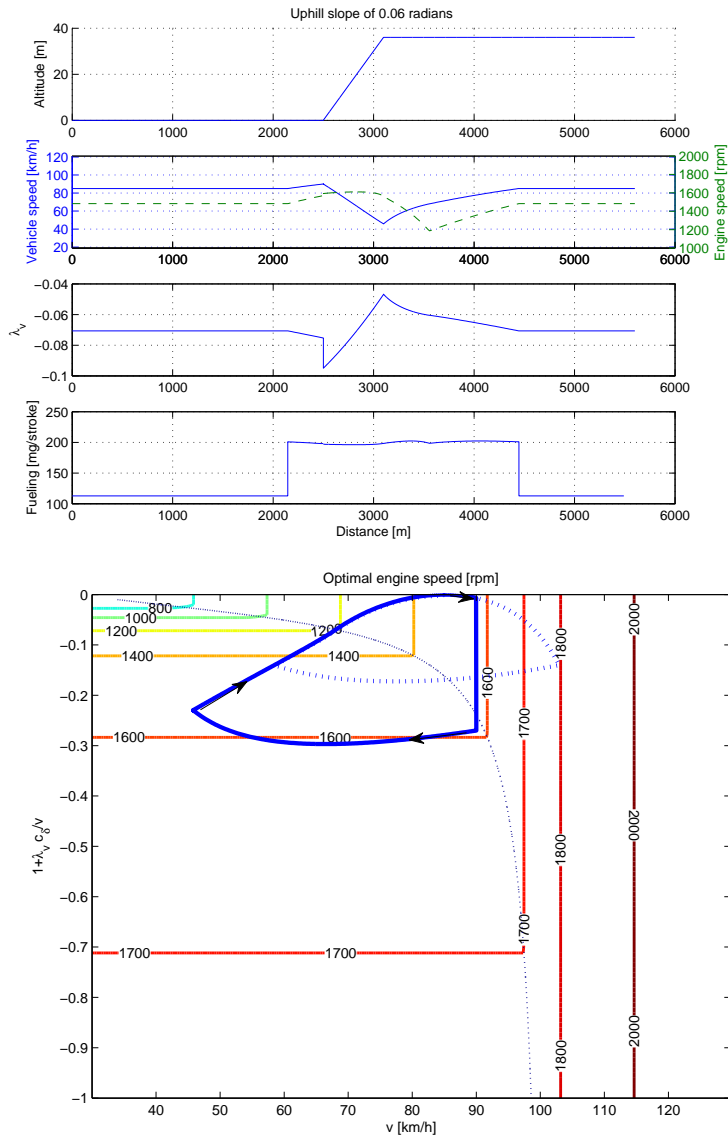


Figure 16: Simulation in a 6 % 600 m uphill slope with maximum allowed speed of 90 km/h, solid line. The unconstrained solution from Figure 13 of the same simulation case is also plotted in the lower plot, dotted line.

Coefficient	Sensitivity, $\alpha = -0.03$ $\delta = 0$ mg/stroke	Sensitivity, $\alpha = 0$ $\delta = 113$ mg/stroke	Sensitivity, $\alpha = 0.03$ $\delta = 220$ mg/stroke
$c_\delta$	0.00	323	-1.48
$c_\omega$	-0.12	-49	0.11
$c_e$	0.079	32	-0.076
$c_c$	-0.42	-171	0.40
$c_v$	0.00	0.00	0.00
$c_{v2}$	-0.33	-135	0.32
$c_\alpha$	1.78	0.00	1.72
$\alpha$	1.78	0.00	1.72

Table 3: Sensivity of vehicle dynamics to model coefficients. The sensitivity is calculated for a 40 ton truck cruising at 85 km/h

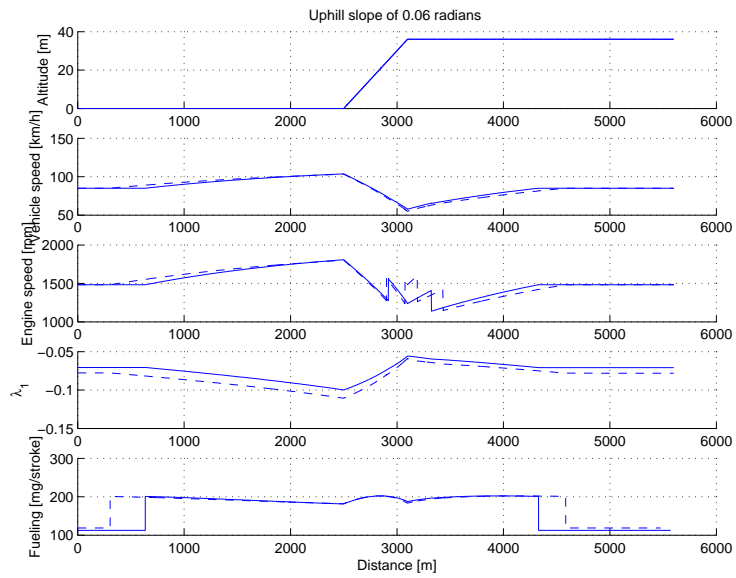


Figure 17: Simulation in a 6 % 600 m uphill slope with masses 44 tons (dashed lines) and 40 tons (solid lines).

extra gear shift which of course gives an increase in fuel consumption. In a downhill slope it is of course also worse to underestimate the mass than to overestimate since an underestimate leads to a later deceleration before the slope, which in turn leads to a higher speed in the slope. In presence of speed limits this leads to unnecessary braking and an increase of total fuel consumption.

## 8 Rule based predictive cruise control

There are several ways to use the presented optimality conditions in attempts towards an on-line controller. Looking at the vehicle dynamics in the time domain, vehicle speed can be solved analytically, as in [2], on constant grades for both constant fueling and maximum fueling. Given the equations for vehicle speed and the constraint on total travel time, the problem of finding optimal controls is that of finding optimal control switching points, by solving a system of nonlinear equations [2].

Another approach to utilize the analytical solutions to the vehicle motion will here be used as part of an on-line predictive cruise controller. One advantage is that the assumption that the road grade is piece-wise constant can be dropped.

To demonstrate the possibility to significantly save fuel using the second approach, a simple rule based predictive cruise controller has been implemented. For simplicity the controller is based on the results using an affine engine torque model as in Section 3. It would be possible to make further improvements using a controller based on non-linear engine characteristics and optimize gear choice. However, the purpose here is only to demonstrate the magnitude of the savings that can be done using the presented material. In [6] the possible savings of gear choice is presented.

### 8.1 Optimization criterion

The idea for an on-line controller is to locate upcoming steep hills, compare different fueling strategies with respect to a criterion over a prediction horizon, use the best strategy over a sampling distance, and then re-evaluate the criterion at the next sampling point. Closed loop control is achieved by recalculating optimal controls at every sample point.

An idea for criterion could be to use the Hamiltonian (9). Over short horizons it might however not be a good idea to try to control the average speed to a given value. For example, if the road mostly consists of downhill slopes during the prediction horizon it is often better for the total driving mission to have a higher speed than average, and the opposite for sections of mostly uphill slopes. Influenced by (9) the criterion for a prediction horizon from  $s = 0$  to  $s = S_p$  could be chosen as

$$\tilde{J} = \int_0^{S_p} \delta i ds + \lambda_T \int_0^{S_p} f_T ds \quad (65)$$

The first term is proportional to the fuel consumed while driving the distance  $S_p$  and the second term accounts for the travel time. The time penalty  $\lambda_T$  is obtained by solving Equation (14) using a desired stationary speed  $v_{ref}$  on flat roads and small gradients. For this criterion to be useful it has to be modified to account for the speed at the end of horizon. As known from Section 3 the optimal solution consists of constant speed, maximum fueling, and fuel cut off. Using (65) will result in a strategy that uses fuel cut off at the end of the prediction horizon.

**Handling residual cost at end of horizon.** One way to deal with this could be to constrain the solution to a given speed, e.g.  $v(S_p) = v_{ref}$ , at the end of the horizon. However, this is not a good idea if for example the end of horizon is in a slope. The way chosen here to deal with the problem of finite horizon is as follows: Assume flat road after  $S_p$ , let  $S_{vref}$  be the position where the reference speed  $v_{ref}$  is reached after  $S_p$  when using either maximum fueling or fuel cut off depending on if the speed at  $S_p$  is less than or greater than  $v_{ref}$ . By defining a function  $\Delta$  as

$$\Delta = \int_{S_p}^{S_{vref}} \delta i ds + \lambda_T \int_{S_p}^{S_{vref}} f_T ds \quad (66)$$

the criterion (65) can be chosen as

$$J = \int_0^{S_p} \delta i ds + \lambda_T \int_0^{S_p} f_T ds + \Delta \quad (67)$$

The function  $\Delta$  then follows from the solution to the vehicles longitudinal dynamics. When using fuel cut off on flat road the vehicle dynamics (7) in the time domain becomes

$$\dot{v} = c_e i + c_c + (c_\omega \frac{i^2}{r} + c_v) v + c_{v2} v^2 \quad (68)$$

Using maximum fueling modeled as  $\delta_{max} = c_{con} + c_{\omega con} \frac{i}{r} + c_{\omega 2 con} \frac{i^2}{r^2}$  results in

$$\dot{v} = c_\delta i c_{con} + c_e i + c_c + (c_\delta c_{\omega con} \frac{i^2}{r} + c_\omega \frac{i^2}{r} + c_v) v + (c_\delta c_{\omega 2 con} \frac{i^3}{r^2} + c_{v2}) v^2 \quad (69)$$

Both Equation (68) and (69) are in the form

$$\dot{v} = c_0 + c_1 v + c_2 v^2 \quad (70)$$

This differential equation can be solved by separating variables as

$$\frac{1}{c_0 + c_1 v + c_2 v^2} dv = dt, \quad c_0 + c_1 v + c_2 v^2 \neq 0 \quad (71)$$

Integrating both sides give

$$\int \frac{1}{c_0 + c_1 v + c_2 v^2} dv = \int dt \quad (72)$$

This equation has two different solutions depending on the coefficients. When accelerating the coefficients are such that the solution to (72) is

$$\frac{1}{\sqrt{-4c_2 c_0 + c_1^2}} \ln \left| \frac{2c_2 v + c_1 - \sqrt{-4c_2 c_0 + c_1^2}}{2c_2 v + c_1 + \sqrt{-4c_2 c_0 + c_1^2}} \right| = t + k \quad (73)$$

The solution to this equation is

$$v(t) = \frac{-(c_1 - \sqrt{c_1^2 - 4c_0 c_2}) - (c_1 + \sqrt{c_1^2 - 4c_0 c_2}) e^{\sqrt{c_1^2 - 4c_0 c_2}(t+k)}}{2c_2 e^{\sqrt{c_1^2 - 4c_0 c_2}(t+k)} + 2c_2} \quad (74)$$

and  $k$  is chosen such that initial conditions are satisfied. When decelerating the coefficients are such that the solution to (72) is

$$\frac{2}{\sqrt{4c_0c_2 - c_1^2}} \arctan \left( \frac{2c_2v + c_1}{\sqrt{4c_0c_2 - c_1^2}} \right) = t + k \quad (75)$$

and also here  $k$  is determined by initial conditions. The vehicle speed given by this equation is

$$v(t) = \frac{1}{2c_2} \left( \sqrt{4c_0c_2 - c_1^2} \tan \left( \frac{\sqrt{4c_0c_2 - c_1^2}}{2} (t + k) \right) - c_1 \right) \quad (76)$$

Now, from (73) or (75) the time required for  $v$  to reach  $v_{ref}$  can be calculated. Given time, distance can be calculated by integrating speed. The distance traveled,  $s = \int v dt$ , during acceleration to  $v_{ref}$ , is given from the integral of (74) which is

$$\begin{aligned} \int \frac{-(c_1 - \sqrt{c_1^2 - 4c_0c_2}) - (c_1 + \sqrt{c_1^2 - 4c_0c_2}) e^{\sqrt{c_1^2 - 4c_0c_2}(t+k)}}{2c_2 e^{\sqrt{c_1^2 - 4c_0c_2}(t+k)} + 2c_2} dt \\ = \frac{\sqrt{c_1^2 - 4c_0c_2} - c_1}{2c_2} t - \frac{\ln \left| 2c_2 (e^{\sqrt{c_1^2 - 4c_0c_2}(k+t)} + 1) \right|}{c_2} \end{aligned} \quad (77)$$

and the distance traveled during deceleration to  $v_{ref}$  is given from the integral of (76) which is

$$\begin{aligned} \int \left( \frac{\sqrt{4c_0c_2 - c_1^2}}{2c_2} \tan \left( \frac{\sqrt{4c_0c_2 - c_1^2}}{2} (t + k) \right) - \frac{c_1}{2c_2} \right) dt \\ = -\frac{c_1}{2c_2} t - \frac{\ln \left| \cos \left( \frac{\sqrt{4c_0c_2 - c_1^2}}{2} (t + k) \right) \right|}{c_2} \end{aligned} \quad (78)$$

Now  $\Delta$ , (66), can be calculated as follows. Given distance the first integral is easily calculated for the different cases of fuel cut off and maximum fueling. The second integral is simply traveled time as given by Equations (73) and (75).

## 8.2 On-line algorithm

Given the results above, an on-line cruise controller can be formulated. For simplicity, as in [6] the standard cruise controller will be used as actuator. When constant speed is desired,  $v = v_{ref}$  is commanded, when maximum fueling is desired, a higher speed than the vehicles present speed will be commanded, and, when fuel cut off is desired, a lower speed than the present speed is commanded. Since the standard cruise controller is of a PID-controller type this strategy will not always lead to the desired fueling but as will be shown in simulations it will be close to desired behavior.

For a realistic case speed, limits has to be imposed such that  $V_{min} \leq v \leq V_{max}$ . The algorithm is as follows:

1. Check if there are steep slopes within the horizon. If not, send  $v_{ref}$  to the cruise controller.
2. If a steep slope is detected, perform two simulations of the vehicle. First simulation: If the first steep slope is an uphill(downhill) slope start using maximum(minimum) fueling and simulate until either  $v_{ref}$  or  $V_{max}(V_{min})$  is reached. Second simulation: Command constant speed on one sample and then use maximum(minimum) fueling.
3. If  $V_{max}(V_{min})$  is reached before  $v_{ref}$  is reached after the slope, command  $v_{ref}$  to the cruise controller.
4. Compare the two solutions by the performance index (67). Chose control according to the simulation with lowest value of the performance index.

This algorithm is implemented in a simulation environment developed by Erik Hellström [4].

Results from the simulations are shown in Figures 18 - 20. There the above rule-based look-ahead cruise controller, LC, is compared to a standard PID-type cruise controller, CC. The allowed speed range is  $80 \leq v \leq 90$  km/h and the reference speed is 85 km/h. The standard cruise controller will not apply the brakes until the upper speed limit is reached. The prediction horizon for the look-ahead controller was set to 1000 m and the sample distance to 50 m. It is seen that the algorithm works as expected from Section 3. In Figure 18 the algorithm starts to accelerate using maximum fueling about 300 m before the slope. The higher speed compared to the standard cruise controller also results in a shorter period on a lower gear. Due to higher average speed for the look ahead cruise controller the fuel consumption is slightly higher compared to the standard cruise controller. However, the trip time is significantly lower. A down hill slope is presented in Figure 19. The look ahead algorithm cut offs the fuel injection and starts to decelerate about 200 m before the slope. This results in a shorter period of braking and significant fuel savings but a small increase in trip time. For a real road consisting of both uphill slopes and downhill slopes, it is expected that the difference in total travel time between the look ahead cruise controller and the standard cruise controller is moderate. In Figure 20 it is seen that even though the travel time is almost the same for the two controllers the fuel saving is significant for the look ahead controller. It can also be mentioned that the magnitude of the savings is promising even though not quite as high as those reported in [4] using a more sophisticated numerical optimal controller.

## 9 Conclusions

Analytical expressions for optimality of the fuel optimal cruise control problem have been derived. These expressions are essential for the understanding of the decisive parameters affecting fuel optimal driving, and the analytical optimality conditions makes it possible to see how each parameter affects the optimal solution. It has been shown that the expression  $1 + \frac{\lambda_v c_\delta}{v}$  is decisive for both optimal fueling and optimal gear selection. For example, it is seen in Equation (12) that the ratio between engine torque to vehicle mass, given by the parameter  $c_\delta$ , directly affects the optimal control switch points, which also the adjoint variable  $\lambda_v$  and vehicle speed  $v$  does. The adjoint variable  $\lambda_v$  reacts to future changes in road slope and from that the control switch points

given by (12) also depends on road inclination. This type of analysis lead to the idea of using phase plots with  $1 + \frac{\lambda_v c_{\delta}}{v}$  and  $v$  on the axes, and this type of plot has been used extensively, see Figures 6, 7, 13, 14, and 16. It has also been shown that, accounting for small non-linearities in the engine torque model, fueling is gradually increased or decreased to the fueling limit, giving a smoother control than achieved for an affine model, see for example Figure 11. This gradual change in control also means that a longer prediction horizon is needed.

The maximum fueling function has strong influence on optimal gear choice. It is shown for a continuously variable transmission that it is never optimal to operate above the engine speed of maximum engine power. Further, for typical cases, see Figure 13, during the acceleration phase before an uphill slope it is never optimal to shift gear, but it can be optimal to stay at a higher gear ratio for a short distance after the slope. From the results in Figure 13 it is seen that for optimal solutions engine speed is approximately constant during the slope, and is determined by the vehicle speed at the beginning of the slope. The optimal vehicle speed at the beginning of the slope mostly depends on the length and inclination of the slope and hence optimal gear shifting is approximately a function of slope length and inclination. Another point to notice is that for non-linear fuel-torque characteristics, in order to avoid inefficient engine operating points, it can be beneficial to shift gear instead of using maximum fueling.

Optimal solutions for a discrete stepped transmission are close to the continuous gear ratio solutions in the sense that engine speed for the two cases are close. However, it is shown in simulations that modeling of gear shifting losses are important for gear shifting positions.

The theory presented is a good base to formalize the intuition of fuel efficient driving and one example where the analytical optimality expressions can be used is in design of a simple low-complexity computationally efficient rule-based controller. Such a controller has been shown to be able to save a large part of the possible savings achieved with more computationally demanding controllers based on numerical optimization.

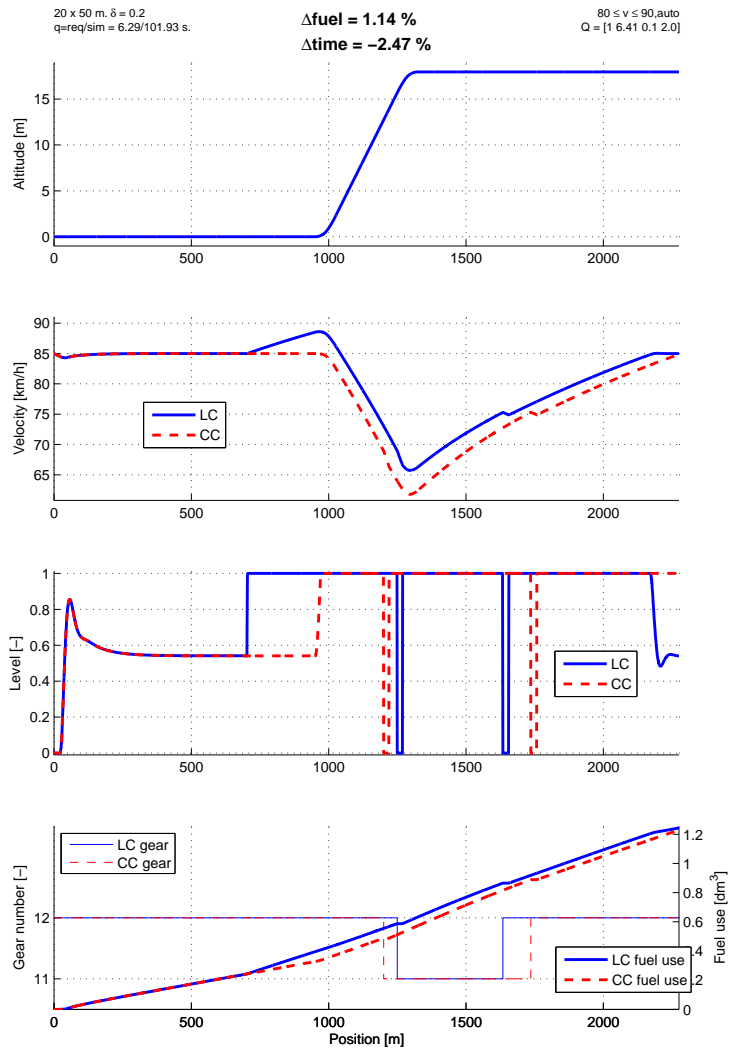


Figure 18: Rule based algorithm in a 6 % 300 m uphill slope. LC denotes Look-ahead cruise controller and CC denotes the standard cruise controller.

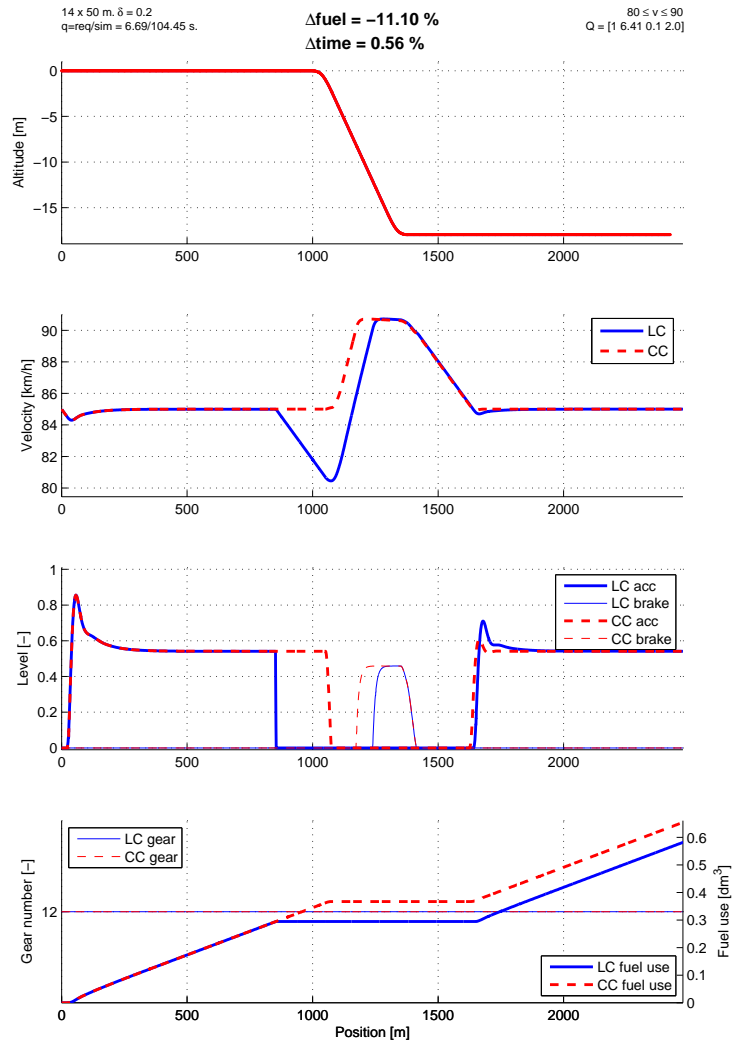


Figure 19: Rule based algorithm in a -6 % 300 m downhill slope. LC denotes Look-ahead cruise controller and CC denotes the standard cruise controller.

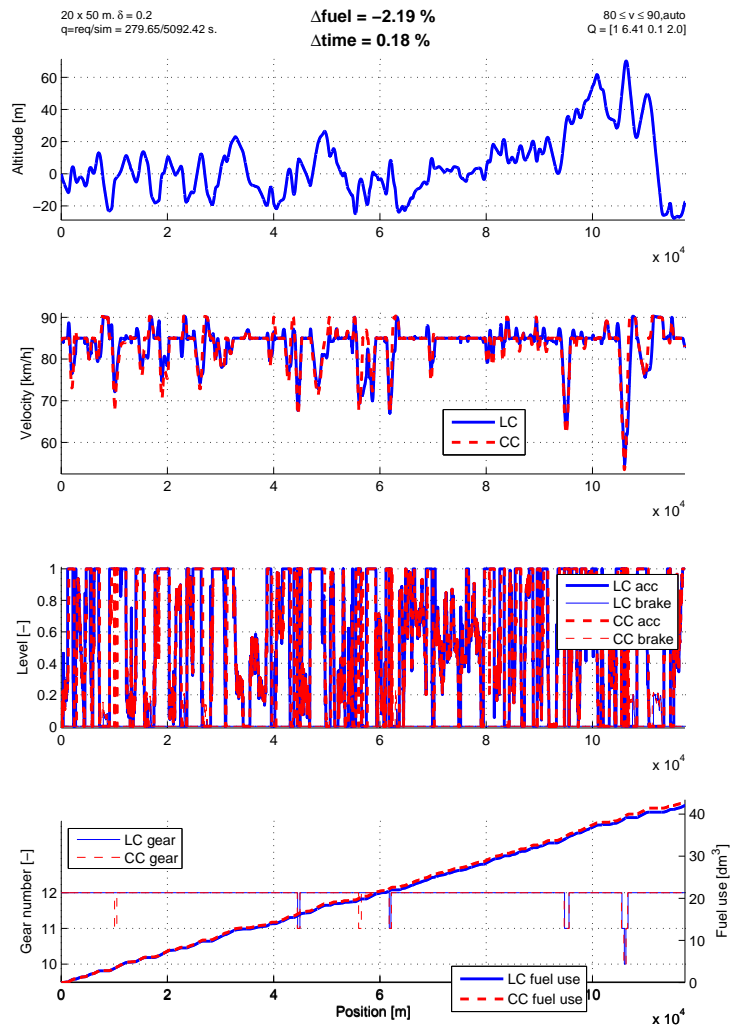


Figure 20: Simulation of the rule based algorithm on the Highway E4 between the cities Södertälje and Norrköping in Sweden. LC denotes Look-ahead cruise controller and CC denotes the standard cruise controller.

## References

- [1] Arthur E. Bryson and Yu-Chi Ho. *Applied optimal control*. Taylor and Francis, 1975.
- [2] A. Fröberg, E. Hellström, and L. Nielsen. Explicit fuel optimal speed profiles for heavy trucks on a set of topographic road profiles. *SAE Technical Paper Series*, 2006-01-1071, 2006.
- [3] Anders Fröberg and Lars Nielsen. Optimal fuel and gear ratio control for heavy trucks with piece wise affine engine characteristics. Fifth IFAC symposium on advances in automotive control, Monterey Coast, California, 2007.
- [4] Erik Hellström. *Look-ahead control of heavy trucks utilizing road topography*. Licentiate thesis, LIU-TEK-LIC-2007:28, Linköping Institute of Technology, Linköping, 2007.
- [5] Erik Hellström, Jan Åslund, and Lars Nielsen. Design of a well-behaved algorithm for on-board look-ahead control. *IFAC World Congress, Korea*, 2008.
- [6] Erik Hellström, Maria Ivarsson, Jan Åslund, and Lars Nielsen. Look-ahead control for heavy trucks to minimize trip time and fuel consumption. Fifth IFAC Symposium on Advances in Automotive Control, Monterey, CA, USA, 2007.
- [7] J.N. Hooker. Optimal driving for single-vehicle fuel economy. *Transportation Research part a*, 22(3), May 1988.
- [8] Maria Ivarsson, Jan Åslund, and Lars Nielsen. Optimal speed on small gradients - consequences of a non-linear fuel map. *IFAC World Congress, Korea*, 2008.
- [9] U. Kiencke and L. Nielsen. *Automotive Control Systems, 2nd ed.* Springer-Verlag, 2005.
- [10] F. Lattemann, K. Neiss, S. Terwen, and T. Connolly. The predictive cruise control - a system to reduce fuel consumption of heavy duty trucks. *SAE Technical paper series*, (2004-01-2616), 2004.
- [11] George Leitmann. *The calculus of variations and optimal control*. Plenum press, 1981.
- [12] Rongfang Liu and Iakov M. Golovitcher. Energy -efficient operation of rail vehicles. *Transportation research Part A*, 37(10):917–932, 2003.
- [13] C. Manzie, H. Watson, and S. Halgamuge. Fuel economy improvements for urban driving: Hybrid vs. intelligent vehicles. *Transportation Research Part C*, (15):1–16, 2007.
- [14] S. M. Savaresi, F. L. Taroni, F. Previdi, and S. Bittanti. Control system design on a power-split cvt for high-power agricultural tractors. *IEEE/ASME Transactions on mechatronics*, 9(3):569–579, 2004.
- [15] A. B. Schwarzkoopf and R. B. Leipnik. Control of highway vehicles for minimum fuel consumption over varying terrain. *Transportation Research*, 11:279–286, 1977.

- [16] A. Sciarretta and L. Guzzella. Fuel-optimal control of rendezvous maneuvers for passenger cars. *Automatisierungstechnik*, 53(6):244–250, 2005.
- [17] P. Setlur, J. R. Wagner, D. M. Dawson, and B. Samuels. Nonlinear control of a continuously variable transmission (cvt). *IEEE Transactions on control systems technology*, 11(1):101–108, 2003.
- [18] S. Terwen, M. Back, and V Krebs. Predictive powertrain control for heavy duty trucks. *First IFAC Symposium on Advances in Automotive Control*, 2004.